

# Molecular Basis for Regulation of the Heat Shock Transcription Factor $\sigma^{32}$ by the DnaK and DnaJ Chaperones

Fernanda Rodriguez,<sup>1,3</sup> Florence Arsène-Ploetze,<sup>1,4</sup> Wolfgang Rist,<sup>1,5</sup> Stefan Rüdiger,<sup>1,6</sup> Jens Schneider-Mergener,<sup>2</sup> Matthias P. Mayer,<sup>1,\*</sup> and Bernd Bukau<sup>1,\*</sup>

<sup>1</sup>Zentrum für Molekulare Biologie der Universität Heidelberg, DKFZ-ZMBH Alliance, Im Neuenheimer Feld 282, 69120 Heidelberg, Germany

<sup>2</sup>Institut für Medizinische Immunologie, Universitätsklinikum Charité, Schumannstrasse 20-21, 10098 Berlin, Germany, and the Jerini AG, Invalidenstrasse 130, 10115 Berlin, Germany

<sup>3</sup>Present address: Growth and Development, Biozentrum, University of Basel, Klingelbergstrasse 50/70, CH-4056 Basel, Switzerland

<sup>4</sup>Present address: UMR7156, Université Louis Pasteur/CNRS, Laboratoire de Génétique Moléculaire, Génomique et Microbiologie, Département Micro-organismes, Génomes, Environnement, 28, rue Goethe, 67083 Strasbourg Cedex, France

<sup>5</sup>Present address: Boehringer Ingelheim Pharma GmbH, Department of Respiratory Research, Proteomics Laboratory, Birkendorfer Strasse 65, 88397 Biberach, Germany

<sup>6</sup>Present address: Cellular Protein Chemistry, Department of Chemistry, Utrecht University, Kruytgebouw, Room O-701, Padualaan 8, 3584CH, Utrecht, the Netherlands

\*Correspondence: m.mayer@zmbh.uni-heidelberg.de (M.P.M.), bukau@zmbh.uni-heidelberg.de (B.B.)

DOI 10.1016/j.molcel.2008.09.016

## SUMMARY

Central to the transcriptional control of the *Escherichia coli* heat shock regulon is the stress-dependent inhibition of the  $\sigma^{32}$  subunit of RNA polymerase by reversible association with the DnaK chaperone, mediated by the DnaJ cochaperone. Here we identified two distinct sites in  $\sigma^{32}$  as binding sites for DnaK and DnaJ. DnaJ binding destabilizes a distant region of  $\sigma^{32}$  in close spatial vicinity of the DnaK-binding site, and DnaK destabilizes a region in the N-terminal domain, the primary target for the FtsH protease, which degrades  $\sigma^{32}$  in vivo. Our findings suggest a molecular mechanism for the DnaK- and DnaJ-mediated inactivation of  $\sigma^{32}$  as part of the heat shock response. They furthermore demonstrate that DnaK and DnaJ binding can induce conformational changes in a native protein substrate even at distant sites, a feature that we propose to be of general relevance for the action of Hsp70 chaperone systems.

## INTRODUCTION

The heat shock response is an evolutionary conserved protective mechanism of cells against stress-induced damage of proteins. In *E. coli*, this response is mediated by the *rpoH* gene product, the heat shock transcription factor  $\sigma^{32}$ , that binds as an alternative  $\sigma$  subunit to the RNA polymerase (RNAP) core enzyme and targets it to the promoters of heat shock genes (Bukau, 1993; Gross, 1996; Yura and Nakahigashi, 1999). Stress-dependent changes in heat shock gene expression are mediated by changes in the activity and stability of  $\sigma^{32}$ . In cells growing at 30°C,  $\sigma^{32}$  is rapidly degraded ( $t_{1/2} < 1$  min) primarily by the membrane-bound

AAA-protease FtsH, which accounts for its very low intracellular levels (10–30 molecules per cell). Upon temperature upshift from 30°C to 42°C, the levels and half-life of  $\sigma^{32}$  increase transiently (induction phase). The induction phase is followed by a shut-off phase during which the synthesis of heat shock proteins is reduced to a new steady-state level. This shut-off results from rapid inactivation and destabilization of  $\sigma^{32}$  (Herman et al., 1995; Kanemori et al., 1999; Straus et al., 1987; Tilly et al., 1989; Tomoyasu et al., 1995).

Genetic and biochemical evidences indicate that the major Hsp70 chaperone in *E. coli*, DnaK, and its cochaperones DnaJ and GrpE play a central role for the adjustment of the steady-state levels of heat shock proteins and the rapid shut-off of the heat shock response (Grossman et al., 1987; Straus et al., 1990; Tilly et al., 1983). In vitro,  $\sigma^{32}$  in its native state is recognized as a substrate by DnaK and its cochaperone DnaJ (Gamer et al., 1992, 1996; Liberek et al., 1992, 1995). The interaction of DnaK with  $\sigma^{32}$  is transient and controlled by DnaK's nucleotide status. In the ADP state, the affinity of DnaK to  $\sigma^{32}$  is high and association and dissociation rates are low, while in the ATP state the affinity is low and association and dissociation rates are high (Gamer et al., 1996; Liberek et al., 1995; Mayer et al., 2000). DnaJ binds  $\sigma^{32}$  with high affinity, and simultaneous interaction of DnaJ and  $\sigma^{32}$  with DnaK·ATP stimulates DnaK's ATPase activity several thousand-fold, leading to the tight binding of DnaK·ADP to  $\sigma^{32}$  (Gamer et al., 1992, 1996; Laufen et al., 1999; Liberek et al., 1995).

The precise mechanism by which DnaK and DnaJ interact with  $\sigma^{32}$  and regulate its activity and stability is still unclear. By screening libraries of peptides derived from many different chaperone substrates, earlier work established the consensus motif that DnaK and DnaJ recognize in substrates. For DnaK it is composed of a core of five amino acids enriched in hydrophobic residues flanked by sequences enriched in positively charged amino acids (Rüdiger et al., 1997). By screening a  $\sigma^{32}$ -derived peptide library for DnaK-binding sites, seven sites were identified within the  $\sigma^{32}$

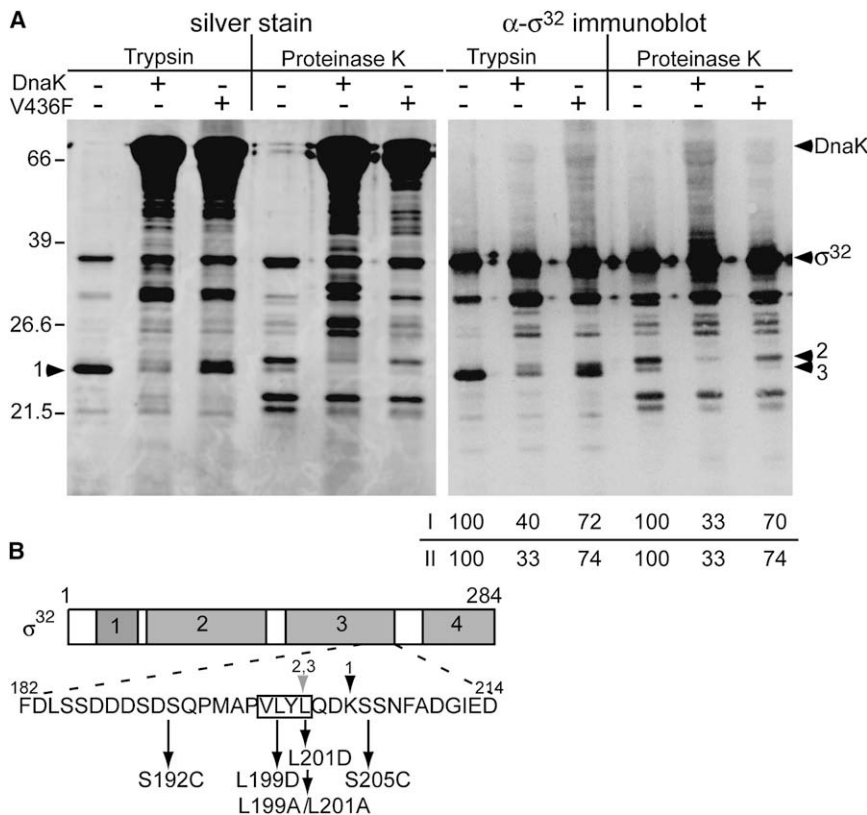


**Figure 1. DnaK Binding Protects Specific Protease Cleavage Sites within  $\sigma^{32}$**

(A) Electrophoretic separation of fragments obtained after partial digestion of the  $\sigma^{32}$  protein by trypsin or Proteinase K in the absence or presence of wild-type DnaK or a DnaK mutant protein (DnaK-V436F) that has a low affinity for  $\sigma^{32}$  (Mayer et al., 2000). Left panel, silver-stained SDS gel; right panel, immunodetection using a  $\sigma^{32}$ -specific polyclonal antiserum. Molecular weight marker indicated to the left. Protected bands are indicated by arrowheads and numbered 1–3. The relative amounts of the protected bands 1 and 2 were quantified using fluorimaging and given as percent of the same band obtained with  $\sigma^{32}$  in the absence of DnaK (I). The theoretical amount of unbound  $\sigma^{32}$  and of  $\sigma^{32}$  released during the incubation time was calculated according to the  $K_D$  and  $k_{off}$  value (II) (Mayer et al., 2000).

(B)  $\sigma^{32}$  is shown schematically with indicated locations of the conserved regions 1–4. Details of the region protected by DnaK are given below the scheme. The black and gray arrowheads indicate the C-terminal residues of the cleavage products 1 (black, K204, trypsin cleavage) and 2 and 3 (gray, L201, Proteinase K cleavage) as determined by MS. The sequences of the potential DnaK-binding site identified by peptide scanning are boxed, and mutational alterations of amino acids introduced into  $\sigma^{32}$  proteins in this study are indicated.

polypeptide sequence (McCarty et al., 1996). However, since this method relies on the analysis of short extended peptides, it remains an open question which of the identified potential binding sites is responsible for the binding of DnaK to the native  $\sigma^{32}$  protein.

For DnaJ, the consensus motif consists of a hydrophobic core of approximately eight residues enriched for aromatic and large aliphatic residues and arginine (Rüdiger et al., 2001). Peptide library scans of  $\sigma^{32}$  have not been reported yet. The similarity of the binding motifs of DnaK and DnaJ allows for the possibility of a direct transfer of a DnaJ bound peptide into DnaK's substrate-binding pocket (Rüdiger et al., 2001).

To understand the heat shock regulation at a molecular level, we set out to identify the regions of  $\sigma^{32}$  directly involved in the DnaK- and DnaJ-mediated control. Furthermore, given that substrates of DnaK and DnaJ usually are nonnative polypeptides, it will be of particular interest to determine the structural features that turn  $\sigma^{32}$  into a native substrate of DnaK and DnaJ. The interaction of DnaK and DnaJ with  $\sigma^{32}$  is considered to be a paradigm for the interaction of Hsp70 chaperones with regulatory native substrates.

In this paper, we report the identification of two different segments within native  $\sigma^{32}$  where DnaK and DnaJ bind. Using amide hydrogen- $^1\text{H}/^2\text{H}$ -exchange (HX) experiments in combination with mass spectrometry (MS), we observed conformational changes in  $\sigma^{32}$  upon DnaK and DnaJ binding. Our results provide mechanistic insights into both the chaperone action of Hsp70 systems and the regulation of the heat shock response.

## RESULTS

### DnaK Binding Protects $\sigma^{32}$ against Proteolytic Cleavage at One Specific Site

The DnaK- $\sigma^{32}$  complex consists of one DnaK molecule bound to one  $\sigma^{32}$  molecule (Gamer et al., 1996; Liberek et al., 1992), suggesting that  $\sigma^{32}$  has only one DnaK-binding site. To map this site within the native  $\sigma^{32}$  protein, we employed a protease footprinting approach, which assumes that DnaK binding prevents proteolytic cleavage of  $\sigma^{32}$  in the neighborhood of its binding site. The most useful cleavage patterns were obtained with trypsin and Proteinase K. Identical fragments were observed for authentic and C-terminal His-tagged  $\sigma^{32}$  (data not shown). To facilitate the interpretation of the  $\sigma^{32}$  cleavage pattern in the presence of DnaK, the bands were detected by immunoblotting using a  $\sigma^{32}$  specific antiserum (Figure 1A). As a negative control, a DnaK mutant protein (DnaK-V436F) that has a 17-fold lower affinity for  $\sigma^{32}$  (Mayer et al., 2000) was included. In the presence of a 5-fold molar excess of DnaK, three  $\sigma^{32}$  bands (1–3 in Figure 1A) were less prominent than in the absence of DnaK or the presence of DnaK-V436F, indicating a protected cleavage site (Figure 1A). The amount of  $\sigma^{32}$  that is protease accessible in the course of the protease digestion assay consists of the unbound equilibrium concentration of  $\sigma^{32}$  and the  $\sigma^{32}$  proteins that are dissociated during the incubation time. The amount of accessible  $\sigma^{32}$  can be calculated on the basis of the known constants of the DnaK- $\sigma^{32}$  interaction: 33% for DnaK wild-type and 74% for DnaK-V436F mutant. Quantification of the bands 1 and 2

**Table 1. Affinity of  $\sigma^{32}$  Wild-Type and Mutant Proteins to DnaK, DnaJ, and RNAP Core Enzyme**

	Dissociation Equilibrium Constants ( $K_D$ )		
	DnaK ( $\mu\text{M}$ ) <sup>a</sup>	DnaJ (nM) <sup>b</sup>	RNAP (nM) <sup>a</sup>
$\sigma^{32}$ -WT	1.4 ± 0.2	21 ± 4	11.6 ± 0.4
$\sigma^{32}$ -L199D	7.1 ± 2.1	ND <sup>c</sup>	65.0 ± 4.9
$\sigma^{32}$ -L201D	8.0 ± 0.5	ND	17.5 ± 1.1
$\sigma^{32}$ -L199A,L201A	11.2 ± 2.5	13 ± 3	758 ± 31

<sup>a</sup>  $K_D$  determined by gel filtration and Scatchard plot analysis.

<sup>b</sup>  $K_D$  determined by SPR.

<sup>c</sup> ND, not determined.

(Figure 1A, panel I) revealed that the cleavage efficiency by trypsin and Proteinase K decreased to 40% and 33%, respectively, in the presence of wild-type DnaK and to 72% and 70% in the presence of DnaK-V436F. The measured protection values thus matched the calculated ones (Figure 1A, panel II).

To identify the trypsin and Proteinase K cleavage sites that are protected by DnaK binding, we analyzed the corresponding fragments of the unprotected  $\sigma^{32}$  by MALDI-TOF MS and N-terminal sequencing (Edman degradation) (Figure 1B). The protected cleavage sites are at positions 204 and 201 of the  $\sigma^{32}$  polypeptide chain for trypsin and Proteinase K, respectively. To verify that DnaK binds to the same site in vivo, we isolated the DnaK- $\sigma^{32}$  complex ex vivo, subjected the complex and isolated  $\sigma^{32}$  for comparison to tryptic digestion, and analyzed the reaction products by high-resolution electrospray MS. A prominent peak from the deconvoluted mass spectrum of the tryptic digest of  $\sigma^{32}$  corresponding to a  $\sigma^{32}$  fragment ending in Lys204 was absent from the mass spectrum of the DnaK- $\sigma^{32}$  complex (see Figure S1 and Table S1 available online). The cleavage sites are adjacent to a single potential DnaK-binding site with a core of four large hydrophobic amino acids (<sup>198</sup>Val-Leu-Tyr-Leu<sup>201</sup>) as experimentally identified by scanning a  $\sigma^{32}$  peptide library (Figure S2). A peptide that contains both cleavage sites ( $\sigma^{32}$ -M195-N207) also binds with high affinity to DnaK in solution (McCarty et al., 1996). This hydrophobic patch (residues 198–201) is the only segment within the entire region that experimentally shows high affinity for DnaK at the peptide level.

### DnaK Binds at Positions 198–201 of $\sigma^{32}$

To evaluate whether the identified site is the DnaK-binding site in folded  $\sigma^{32}$ , the site was mutated and the affinity for DnaK determined. Two key residues of the hydrophobic core of the identified site, leucine 199 and leucine 201, were exchanged to aspartic acid and alanine, respectively, creating the mutant proteins  $\sigma^{32}$ -L199D,  $\sigma^{32}$ -L201D, and  $\sigma^{32}$ -L199A,L201A (Figure 1B). The  $K_D$  for the complex of DnaK with wild-type and mutant  $\sigma^{32}$  was determined by gel filtration. The alterations in the putative DnaK-binding site lowered the affinity for DnaK by 5- to 8-fold (Table 1). Using peptides encompassing the identified DnaK-binding site in wild-type and mutant sequences and measuring their  $K_D$  for binding to DnaK, we could rationalize the observed changes in affinity for DnaK binding to the  $\sigma^{32}$  wild-type and mutant proteins (see the Supplemental Data).

To obtain further evidence for the association of DnaK with the identified site of native  $\sigma^{32}$ , we introduced two cysteines in close

vicinity of the putative DnaK-binding site. We labeled the two  $\sigma^{32}$  cysteine mutant proteins with the heterobifunctional crosslinker BPIA, induced crosslinking by UV treatment in the absence or presence of DnaK, and separated the crosslinking products by SDS-PAGE for immunodetection. With both mutants, we found a crosslinking product of approximately 130 kDa that was immunoreactive to DnaK- and  $\sigma^{32}$ -specific antisera, indicating that the respective cysteines are within 10 Å distance from bound DnaK (see Figure S3 for  $\sigma^{32}$ -S205C). Taken together, these results demonstrate that the identified site is the DnaK-binding site in the native  $\sigma^{32}$  protein.

### DnaK Protects at Least Two Amide Hydrogens in the DnaK-Binding Site of $\sigma^{32}$

To investigate whether DnaK binding induces conformational changes in  $\sigma^{32}$ , we performed HX-MS experiments with  $\sigma^{32}$  free and bound to DnaK. HX-MS is a powerful technique to map protein-protein binding interfaces and conformational changes. The crystal structure of the substrate-binding domain of DnaK in complex with a substrate peptide shows three hydrogen bonds between DnaK and amide hydrogens of the cocrystallized peptide. In addition, one amide hydrogen of the bound peptide is shielded from surrounding water (Zhu et al., 1996). Therefore we would expect a protection of four amide hydrogen in  $\sigma^{32}$  when DnaK is bound. However, HX-MS experiments analyzing full-length  $\sigma^{32}$  in the absence and presence of DnaK showed no differences in the kinetics of deuterium incorporation (Figure S4A). This result can be explained in two alternative ways. Either  $\sigma^{32}$  is bound to DnaK in a way different from the peptide in the crystal structure so that there are no amide hydrogens protected, or protection through DnaK binding is balanced by conformational changes that induce deprotection in a different region of the  $\sigma^{32}$  protein. To distinguish between the two alternatives, we had to localize fast and slow exchanging regions within  $\sigma^{32}$  by peptic digestion under quench conditions after the HX reaction. For reasons explained in more detail in the Supplemental Data, these experiments had to be performed using DnaK immobilized to a column.

To determine the number of amide hydrogens that are protected when a substrate is bound to DnaK, we first performed the HX experiments with the immobilized DnaK and a peptide substrate derived from  $\sigma^{32}$ ,  $\sigma^{32}$ -M195-N207. This peptide contains the DnaK-binding site in the folded  $\sigma^{32}$  protein identified here. The peptide was incubated with immobilized DnaK for 30 min in a column containing either immobilized DnaK or an anion exchange material for control (to allow binding of the peptide in the absence of DnaK). As shown in Figure 2C, when DnaK is bound, four amide hydrogens are protected in the peptide. This is in agreement with the crystal structure of the substrate-binding domain of DnaK in complex with a substrate peptide (Zhu et al., 1996).

The HX experiment was then performed with C-terminally His-tagged  $\sigma^{32}$  protein as substrate on the DnaK column and, for control, on a Ni<sup>2+</sup>-NTA column to immobilize  $\sigma^{32}$  in the absence of DnaK. After different exchange times, the bound  $\sigma^{32}$  was eluted from both columns with low pH quench buffer and subsequently digested using immobilized pepsin. These experiments revealed that three segments exchange less in the presence of

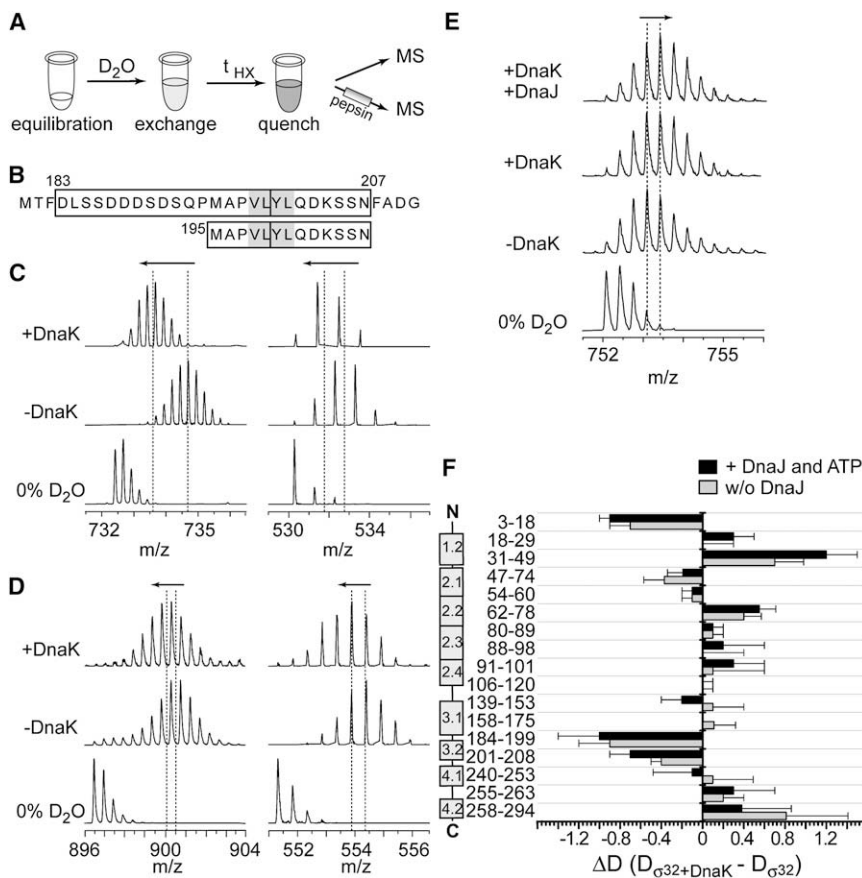


**Figure 2. DnaK Binding to  $\sigma^{32}$  Alters the Deuteron Incorporation into  $\sigma^{32}$**   
(A) Experimental procedure of the HX-MS experiments.

(B) Sequence of  $\sigma^{32}$  (residues 180–211; upper sequence) and of the model peptide  $\sigma^{32}$ -M195-N207 (lower sequence). The DnaK-binding site (gray) and two peptic peptides of  $\sigma^{32}$ , residues 183–199 and 200–207 (boxed), which show a protection of one amide hydrogen each in the presence of DnaK as compared to its absence (D), are indicated in the upper sequence. In the lower sequence are indicated the two peptides (residues 195–199 and 200–207) generated of  $\sigma^{32}$ -M195-N207 upon peptic digestion.

(C) Four amide hydrogens of the model peptide  $\sigma^{32}$ -M195-N207 are protected in the presence of DnaK. Shown are mass spectra of the model peptide  $\sigma^{32}$ -M195-N207 (left panel) and of the peptic fragment residues 195–199 of this peptide (right panel) before incubation in D<sub>2</sub>O or after 30 s in D<sub>2</sub>O in the absence or in the presence of DnaK as indicated. The dashed lines indicate the position of the centroids of the peptide spectra, and the arrows indicate the effect of DnaK binding.

(D) At least two amide hydrogens are protected in  $\sigma^{32}$  through binding of DnaK. Mass spectra of the peptic fragment residues 183–199 (left panel) and 200–207 of  $\sigma^{32}$  (right panel) before incubation in D<sub>2</sub>O or after 30 s in D<sub>2</sub>O in the absence or in the presence of DnaK as indicated.

(E) DnaK binding to  $\sigma^{32}$  destabilizes a region in the N-terminal domain of  $\sigma^{32}$ . Mass spectra of the peptic fragment residues 30–49 of  $\sigma^{32}$  before incubation in D<sub>2</sub>O or after 30 s in D<sub>2</sub>O in the absence or in the presence of DnaK or DnaK and DnaJ as indicated.

(F) Difference plot of deuteron incorporation into  $\sigma^{32}$  in the presence of immobilized DnaK (gray bars) or DnaK, DnaJ, and ATP (black bars) minus deuteron incorporation into  $\sigma^{32}$  in the absence of chaperones (bound to Ni<sup>2+</sup>-NTA). The error bars indicate the standard error of the mean.

DnaK as compared to the absence of DnaK. Two segments are located in the identified DnaK binding site: residues 184–199 and 201–208 (Figures 2D and 2F). Unfortunately, pepsin has a cleavage site in the middle of the hydrophobic DnaK-binding site, explaining the fact that we did not observe four protected hydrogens in that region (the maximum number of two protected amide hydrogens per pepsin-generated peptide is further reduced to one per peptide by the hydrolysis reaction). The same result was obtained when the  $\sigma^{32}$ -M195-N207 peptide was digested with pepsin subsequent to the exchange reaction (Figure 2C, right panel). Time course experiments revealed a protection of these two segments over a time interval of 600 s (Figures S4C and S4D). The probability that the observed differences between the incorporated deuterons in the presence and in the absence of DnaK are merely due to stochastic measurement errors is  $1.8 \cdot 10^{-10}$  and  $9 \cdot 10^{-9}$  for the peptides 183–199 and 200–208, respectively. These results indicate that DnaK binds to  $\sigma^{32}$  in the region 200 and that at least two amide hydrogens are protected by DnaK binding.

The other segment that showed protection when DnaK was bound to  $\sigma^{32}$  is located in the N terminus of  $\sigma^{32}$  in a segment comprising residues 3–18. As shown in the Supplemental Data, the protection of this segment is not caused by direct binding

of DnaK to this site but suggests a DnaK-induced conformational change.

### DnaK Destabilizes a Region in Domain 1.2 of $\sigma^{32}$

A central objective of HX experiments of  $\sigma^{32}$  in complex with DnaK was to investigate whether DnaK can induce conformational changes in  $\sigma^{32}$ . In the HX experiments of  $\sigma^{32}$  together with DnaK, we observed in addition to the protection at the N terminus that the segment 31–49 exchanged more amide protons for deuterons when  $\sigma^{32}$  was bound to DnaK as compared to  $\sigma^{32}$  in the absence of DnaK, suggesting that there is a destabilization of this region upon binding of DnaK (Figures 2E and 2F). This was observed throughout the time course of exchange (Figure S4B). From the kinetics of the exchange, a  $\Delta\Delta G$  value of  $16 \text{ kJ} \cdot \text{mol}^{-1}$  can be calculated (Supplemental Data). This is comparable to the most dramatic amino acid replacement within an  $\alpha$  helix (alanine to proline,  $\Delta\Delta G = 14.5 \text{ kJ} \cdot \text{mol}^{-1}$ ) or the loss of a disulfide bridge ( $\Delta\Delta G \leq 17 \text{ kJ} \cdot \text{mol}^{-1}$ ) (e.g., Blaber et al., 1993; Clarke and Fersht, 1993; Horovitz et al., 1992; O’Neil and DeGrado, 1990; Wetzel et al., 1988). The same effect was observed when  $\sigma^{32}$  was incubated with substoichiometric (1/10<sup>th</sup>) concentrations of DnaJ and excess ATP together with immobilized DnaK (Figures 2E and 2F). This result indicates that, as compared to

free  $\sigma^{32}$ , DnaK-bound  $\sigma^{32}$  is in a different conformation with a more protected region 3–18 and a destabilized region 31–49 both in the N-terminal domain, suggesting that DnaK induces a conformational change in  $\sigma^{32}$ .

### DnaJ and DnaK Bind $\sigma^{32}$ at Different Sites

It was proposed that DnaJ binds to substrates and hands them over to DnaK in a process that is coupled to ATP hydrolysis by DnaK (Han and Christen, 2003; Karzai and McMacken, 1996; Laufen et al., 1999). The DnaJ substrate-binding properties are consistent with two not mutually exclusive modes of action: mode 1 would see DnaK binding to the same site within the substrate as DnaJ before involving a handover step, and mode 2 proposed binding of DnaK and DnaJ to different sites (Rüdiger et al., 2001). To test these two hypotheses, we analyzed the binding sites for DnaJ within  $\sigma^{32}$ , first at the primary structure level using the  $\sigma^{32}$ -derived peptide library (Figure S2). We observed four different continuous series of spots marking potential DnaJ-binding sites in  $\sigma^{32}$ . These correspond to residues 52–64, 88–110, 139–151, and 235–247. None of these sites corresponds to the identified DnaK-binding site in  $\sigma^{32}$  (Figure S2), suggesting that DnaK and DnaJ bind to different sites. This hypothesis is supported by the fact that DnaJ binding was not altered for the  $\sigma^{32}$ -L199A,L201A mutant that shows decreased affinity for DnaK (Table 1). Therefore, DnaK and DnaJ bind to  $\sigma^{32}$  in different regions, and the direct transfer mechanism is not operative in the case of  $\sigma^{32}$ .

### DnaJ Binds in the N-Terminal Domain of $\sigma^{32}$

The peptide library scans indicated at least four possible binding sites in  $\sigma^{32}$ . However, it needs to be established whether these sites expose hydrophobic side chains that may be recognized by DnaJ (Rüdiger et al., 2001) in the context of the native  $\sigma^{32}$  protein. Since DnaJ is known to recognize the hydrophobicity of amino acid side chains rather than the peptide backbone, we needed a structural model, which shows solvent accessibility of side chains, to rationally design truncation and point mutants that would abolish one or several DnaJ-binding sites. Therefore, two different  $\sigma^{32}$  homology models were created based on the crystal structures of *Thermus thermophilus*  $\sigma^{70}$  in complex with RNAP (Vassilyev et al., 2002) and of *Aquifex aeolicus*  $\sigma^{28}$ /FlhA in complex with its anti- $\sigma$ -factor FlgM (Sorenson et al., 2004) and verified with our previous HX-MS analysis of  $\sigma^{32}$  (see Figure S5) (Peitsch, 1996; Rist et al., 2003). Based on these models, we constructed two  $\sigma^{32}$  deletion mutants (Figure 3A): in  $\sigma^{32}$ - $\Delta$ N ( $\sigma^{32}$ -122–284), two of the potential binding sites (sites I and II) were deleted, while in  $\sigma^{32}$ - $\Delta$ C ( $\sigma^{32}$ -2–224) the C-terminal potential binding site (site IV) was deleted. Both deletion mutants bound DnaK with the same affinity as  $\sigma^{32}$  wild-type (data not shown). We then determined the  $K_D$  of these two deletion mutants for DnaJ using surface plasmon resonance spectroscopy (SPR). The  $K_D$  of  $\sigma^{32}$ - $\Delta$ C was similar to the  $K_D$  of  $\sigma^{32}$  wild-type, while that of  $\sigma^{32}$ - $\Delta$ N was 6.5-fold higher (Figure 3C).

It is known that  $\sigma^{32}$  and DnaJ each individually stimulate DnaK's ATP hydrolysis rate, and jointly they stimulate the ATP hydrolysis rate in a synergistic fashion (Laufen et al., 1999). A  $\sigma^{32}$  mutant that cannot bind DnaJ as efficiently as  $\sigma^{32}$  wild-type would be expected to fail in the DnaJ-mediated synergistic

stimulation, but not in the substrate-only stimulation of DnaK's ATPase activity. Single-turnover experiments were performed with  $\sigma^{32}$  wild-type and the two deletion mutants. Both deletion mutants stimulated the ATPase rate of DnaK-like wild-type  $\sigma^{32}$  when they were incubated with DnaK in the absence of DnaJ. In the additional presence of DnaJ,  $\sigma^{32}$ - $\Delta$ C but not  $\sigma^{32}$ - $\Delta$ N stimulated synergistically DnaK's ATP hydrolysis rate like  $\sigma^{32}$  wild-type (Figure 3D). This suggests that the N-terminal deletion mutant is not loaded onto DnaK in an ATP- and DnaJ-dependent manner. This was directly shown in gel filtration experiments (Figure 3E).

To determine which of the two potential binding sites in the N-terminal domain of  $\sigma^{32}$  is the binding site of DnaJ in the folded protein, we created point mutants of these sites and of the two other potential DnaJ-binding sites (sites III and IV) as a control (Figure 3B). In each case, we replaced hydrophobic residues, arginines and histidines, which are centrally located within the hydrophobic core of the putative DnaJ-binding sites and exposed in our homology models, with alanine. Given the substrate-binding specificity of DnaJ (Rüdiger et al., 2001), such mutations are expected to only partially abolish DnaJ binding. We determined the  $K_D$  of these four point mutants to DnaJ using SPR (Figure 3C). Site II, site III, and site IV mutants bound to DnaJ like  $\sigma^{32}$  wild-type. Only the site I mutant showed an increased  $K_D$ . Furthermore, in the absence of DnaJ, all four mutants stimulated the ATP hydrolysis of DnaK like  $\sigma^{32}$  wild-type, indicating that none of the mutants was affected in its interaction with DnaK. A wild-type-like DnaJ-mediated synergistic stimulation of DnaK's ATPase rate, however, was only observed for the mutant in sites II, III, and IV. The site I mutant protein showed a 3-fold decrease in the DnaJ-mediated synergistic stimulation of DnaK's ATPase rate, consistent with the approximately 3.6-fold lower affinity of this mutant protein for DnaJ. Taken together, these results indicate that DnaJ binds to a single specific site in the N-terminal region of  $\sigma^{32}$ .

### Interaction of DnaJ with Substrates

The mode of DnaJ binding to substrates is controversial. Rüdiger et al. used a peptide library approach to analyze the binding determinants of DnaJ-substrate interaction. They found that DnaJ binding is entirely dominated by interaction with amino acid side chains with a strong preference for aromatic amino acids and that the peptide backbone does not seem to play a major role (Rüdiger et al., 2001). In contrast, the crystal structure of a fragment of the yeast DnaJ ortholog Ydj1 shows a cocrystallized peptide substrate bound via six hydrogen bonds, three of which to amides of the peptide backbone (Li et al., 2003). In addition, the two aromatic residues of the substrate peptide are solvent exposed and do not appear to contribute to binding. Thus, according to the peptide library study, DnaJ binding to polypeptide stretches in substrates would not lead to protection of amide hydrogens, while, according to the crystallographic study, significant protection should occur.

To solve this controversial issue, which is relevant to the mode of binding of J proteins to their substrates in a more general sense, we tested whether DnaJ binding to a peptide substrate leads to the protection of backbone amide hydrogens. We first determined the binding parameters for the interaction of DnaJ with the substrate peptide using SPR immobilizing DnaJ as an

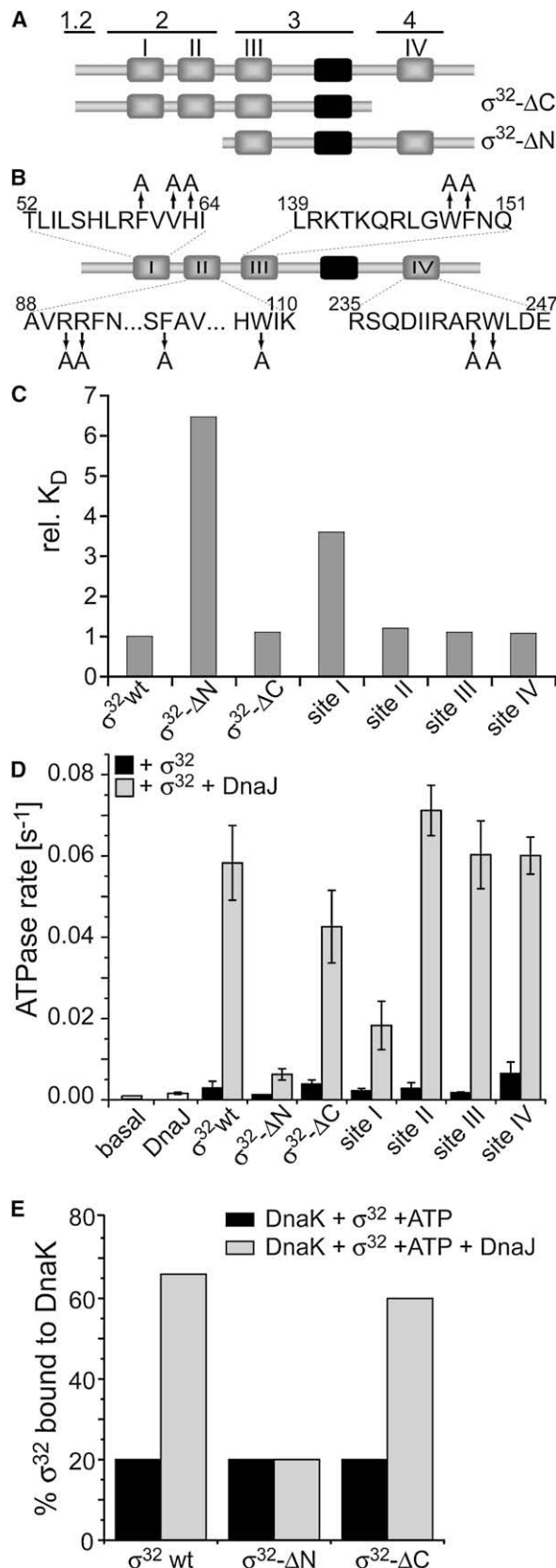


**Figure 3. Point and Deletion Mutant Proteins of  $\sigma^{32}$  Fail to Stimulate the ATPase Rate of DnaK in Synergism with DnaJ**

(A) Schematic representation of  $\sigma^{32}$  and truncation variants ( $\sigma^{32}\text{-}\Delta\text{N}$ ,  $\sigma^{32}\text{-}122\text{-}284$ ;  $\sigma^{32}\text{-}\Delta\text{C}$ ,  $\sigma^{32}\text{-}2\text{-}224$ ) indicating the conserved domains (lines above), the DnaK-binding site (black box), and the potential DnaJ-binding sites as found by peptide library scanning (gray boxes).

(B) Schematic representation of  $\sigma^{32}$  indicating the potential DnaJ-binding sites (gray boxes) and amino acid replacements introduced to disturb binding to DnaJ. Site I,  $\sigma^{32}\text{-F60A,V62A,H63A}$ ; site II,  $\sigma^{32}\text{-R90A,R91A,F104A,W108A}$ ; site III,  $\sigma^{32}\text{-W149A,F150A}$ ; site IV,  $\sigma^{32}\text{-R243A,W244A}$ .

(C) Relative  $K_D$  values for the complexes of DnaJ with wild-type and mutant  $\sigma^{32}$  proteins as determined by SPR.

(D) Single-turnover ATPase rates of DnaK in the presence of  $\sigma^{32}$  wild-type and mutant proteins in the absence (black bars) and presence of DnaJ (gray bars). Basal ATPase rate of DnaK in the absence of any stimulatory protein and DnaJ-stimulated ATPase rate in the absence of  $\sigma^{32}$  are shown in white bars. The error bars indicate the standard deviation of at least three independent determinations.

(E)  $\sigma^{32}\text{-}\Delta\text{N}$  is not loaded onto DnaK in an ATP- and DnaJ-dependent manner.  $^3\text{H}\text{-}\sigma^{32}$  wild-type and truncation variant ( $1\ \mu\text{M}$ ) were incubated with DnaK ( $5\ \mu\text{M}$ ) in the presence of ATP ( $2\ \text{mM}$ ) and in the absence or presence of DnaJ ( $0.2\ \mu\text{M}$ ) for 30 min and subsequently subjected to gel filtration on a Superdex 200 column.

in vivo biotinylated N-terminal fusion protein to biotin carboxyl carrier protein (Figure S6). We then performed with this peptide HX experiments in solution in the absence and presence of DnaJ under conditions in which more than 80% of the peptide remains bound to DnaJ throughout the exchange reaction (Figure 4A). We could not detect any protection of substrate amide hydrogens by the presence of DnaJ. DnaJ therefore does not form hydrogen bonds to the amide hydrogens of the substrate peptide backbone but more likely relies on the interaction with the side chains of hydrophobic residues.

### DnaJ-Bound $\sigma^{32}$ Is Destabilized

To investigate whether the binding of DnaJ alone, in the absence of DnaK, influences the conformation of  $\sigma^{32}$ , we performed HX-MS experiments comparing  $\sigma^{32}$  with  $\sigma^{32}$  in complex with DnaJ. These experiments were performed in solution, since under the conditions used DnaJ was not extensively digested by pepsin, which allowed us to observe the majority of  $\sigma^{32}$  peptides even in the presence of DnaJ. Since the  $K_D$  of the  $\sigma^{32}\text{-DnaJ}$  complex is about 21 nM, under the experimental conditions of  $0.6\ \mu\text{M}$   $\sigma^{32}$  and  $1\ \mu\text{M}$  DnaJ, 95% of  $\sigma^{32}$  was in complex with DnaJ at equilibrium.

To determine the overall amide hydrogen accessibility of DnaJ-bound  $\sigma^{32}$ , we performed the HX-MS experiments first without online peptic digestion after the exchange reaction. The DnaJ- $\sigma^{32}$  complex was incubate for 2–60 s in  $\text{D}_2\text{O}$  and subsequently analyzed in our HPLC-MS setup using gradient elution to separate DnaJ from  $\sigma^{32}$ . As shown in Figure 4B,  $\sigma^{32}$  exchanges more amide hydrogens in the presence of DnaJ than in its absence. A biexponential rate equation was fitted to the data. The fitting results revealed that, in the absence of DnaJ, 150 amide hydrogens exchange at a rate of  $1.13\ \text{s}^{-1}$  and 41 at a rate of  $0.026\ \text{s}^{-1}$ . In the presence of DnaJ, 159 amide hydrogens exchanged at a rate of  $1.32\ \text{s}^{-1}$  and 31 at a rate of  $0.037\ \text{s}^{-1}$ . Since the HX reaction occurred according to the EX2 exchange

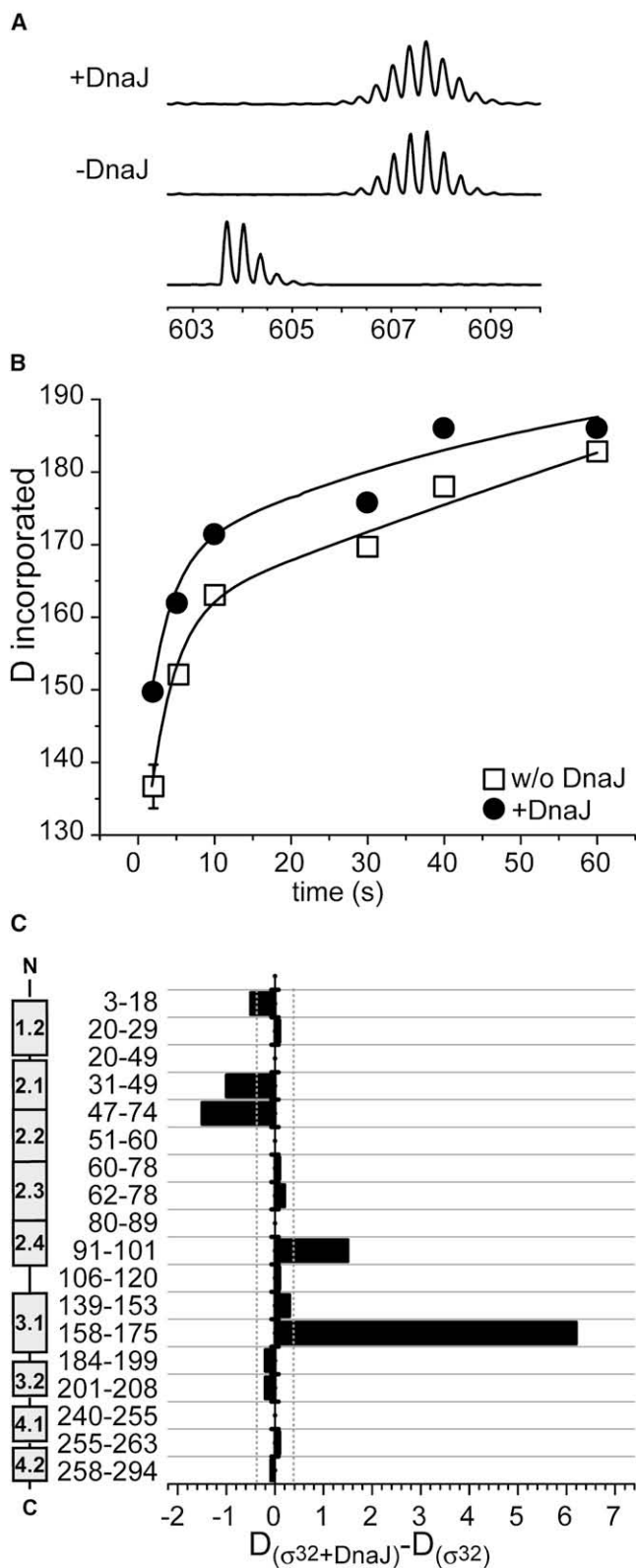


**Figure 4. DnaJ Alters the Deuteron Incorporation Kinetics into  $\sigma^{32}$**   
(A) DnaJ binding to a peptide substrate does not lead to a protection of backbone amide hydrogens. Mass spectra of the peptide  $\sigma^{32}$ -Q132-Q144

mechanism (Hoofnagle et al., 2003), the difference in stability of  $\sigma^{32}$  in the presence and absence of DnaJ ( $\Delta\Delta G$ ) can be estimated from these values. In the presence of DnaJ, nine amide hydrogens more than in the absence of DnaJ exchanged with the fast rate of  $1.3 \text{ s}^{-1}$ . We can assume that these nine amide hydrogens exchanged in the absence of DnaJ with the lower rate of  $0.026 \text{ s}^{-1}$  because the number of amide hydrogens, which exchanged in the presence of DnaJ with the lower rate, was smaller by ten than in the absence of DnaJ. An acceleration of the exchange rate from  $0.026 \text{ s}^{-1}$  to  $1.3 \text{ s}^{-1}$  for nine amide hydrogens results in a large  $\Delta\Delta G$  of  $86 \text{ kJ}\cdot\text{mol}^{-1}$ . This result indicates that DnaJ binding destabilizes  $\sigma^{32}$ .

### DnaJ Opens $\sigma^{32}$ Next to the DnaK-Binding Site

To map the region where DnaJ destabilizes  $\sigma^{32}$ , the HX experiments were repeated by subjecting the protein mixtures after HD exchange to pepsin digestion prior to MS analysis. We found that protection, as well as deprotection, contributes to the overall exchange kinetics of  $\sigma^{32}$  in the presence of DnaJ (Figure 4C). One segment of  $\sigma^{32}$  (residues 47–51) exchanges less amide hydrogens when DnaJ is bound to  $\sigma^{32}$ . This region is close to the identified DnaJ-binding site (residues 57–63). We did not find a protection in the actual DnaJ-binding site. Since HX experiments can only observe the exchange of backbone amide hydrogens, these observations are consistent with our experiments with a model peptide and DnaJ binding exclusively to amino acid side chains as suggested by library-scanning experiments (Rüdiger et al., 2001). We also observed that two segments (residues 91–101 and 158–175) exchanged more amide hydrogens when  $\sigma^{32}$  was bound to DnaJ (Figure 4C) than in the absence of DnaJ. The segment 158–175 is located close in sequence to the DnaK-binding site, and segment 91–101 is located in spatial vicinity of the DnaK-binding site in our  $\sigma^{32}$  homology model that is based on the *A. aeolicus*  $\sigma^{28}$  structure (Figure 5). These findings indicate that DnaJ induces a local opening of the  $\sigma^{32}$  structure. Such an opening could render the DnaK-binding site more accessible, a mechanism that would explain the efficient delivery of  $\sigma^{32}$  to DnaK by DnaJ and why DnaJ and  $\sigma^{32}$  stimulate the ATP hydrolysis rate of DnaK synergistically.

Sequence alignments indicate that the DnaK- and DnaJ-binding sites are conserved in many even distantly related  $\sigma^{32}$  proteins, but not in other  $\sigma$ -factors (Supplemental Data).

### DISCUSSION

In this study, we characterized the interaction of the DnaK-DnaJ chaperone system with  $\sigma^{32}$  at the molecular level. We identified

(QRKLFNLRKTKQ) before and after  $D_2O$  incubation in the absence and presence of DnaJ as indicated.

(B) Kinetics of deuteron incorporation into full-length  $\sigma^{32}$  in the absence (open squares) and presence of DnaJ (black circles). The curves are fits of a biexponential rate equation  $y = A_1[1 - \exp(-k_1t)] + A_2[1 - \exp(-k_2t)]$  to the data with  $A_1$ ,  $k_1$ ,  $A_2$ , and  $k_2$  equal to  $150.0 \pm 2.6$ ,  $1.13 \pm 0.08$ ,  $41.3 \pm 6.7$ , and  $0.026 \pm 0.011$  for the lower curve in the absence of DnaJ and  $158.7 \pm 3.0$ ,  $1.32 \pm 0.12$ ,  $31.1 \pm 3.5$ , and  $0.037 \pm 0.016$  for the upper curve in the presence of DnaJ, respectively. (C) Difference plot of deuteron incorporation into  $\sigma^{32}$  in the presence of DnaJ minus the absence of DnaJ. The gray dotted lines indicate the standard error of the experiment.

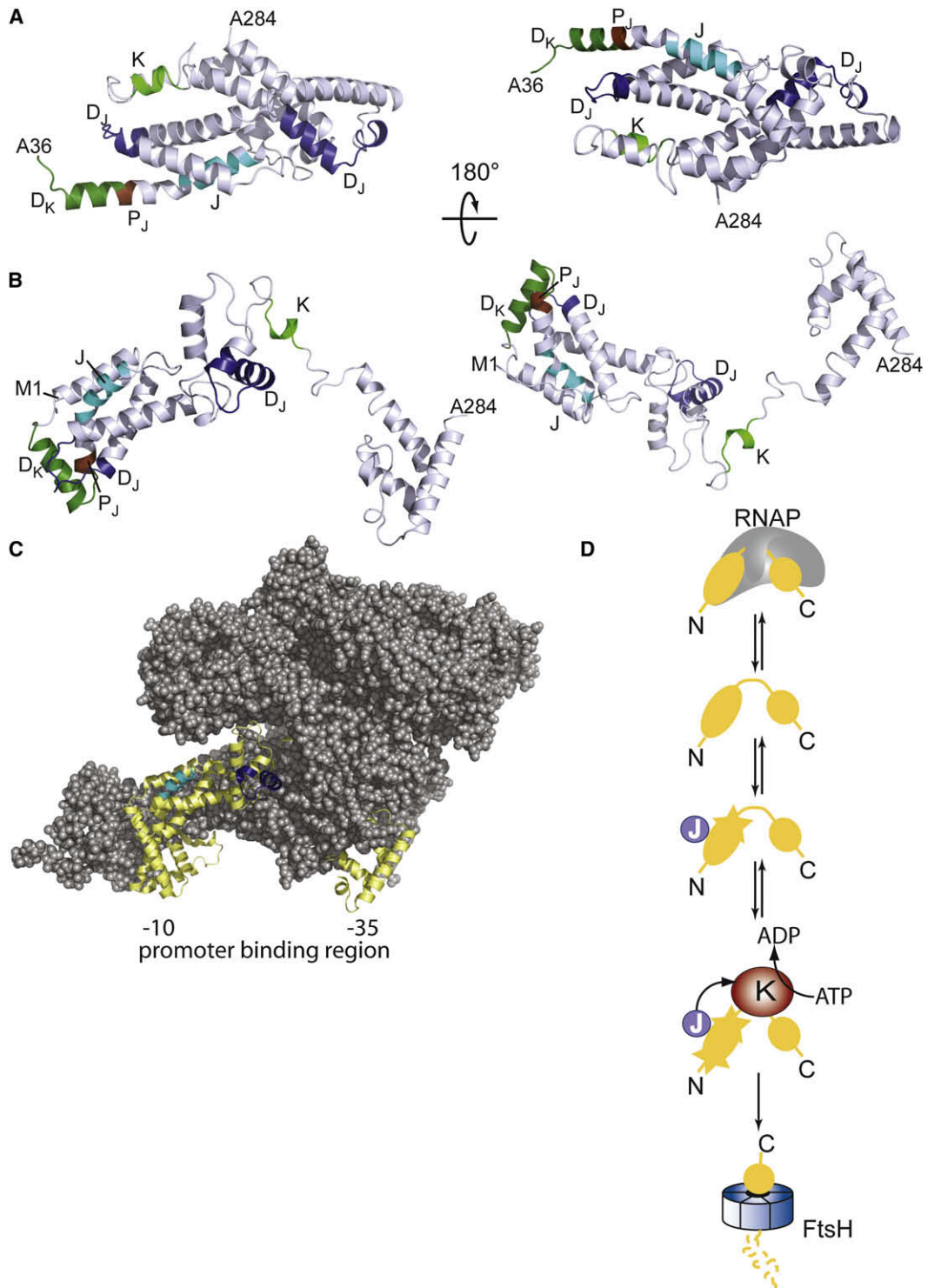


**Figure 5. Molecular Models of DnaK and DnaJ Binding to  $\sigma^{32}$**

Secondary structure representations of homology models of  $\sigma^{32}$  onto *A. aeolicus*  $\sigma^{28}$  (Protein Data Bank [PDB] ID code 1RP3, Sorenson et al. [2004]) (A) and *T. thermophilus*  $\sigma^{70}$  (PDB ID code 1IW7, Vassylyev et al. [2002]) (B) (Peitsch, 1996). The DnaK (K)- and DnaJ (J)-binding sites are colored in green and cyan, respectively. The sites destabilized by DnaK (D<sub>K</sub>) and DnaJ (D<sub>J</sub>) are shown in dark green and dark blue. The site protected by DnaJ binding (P<sub>J</sub>) is shown in brown. The start and end residues of the models are indicated. The right panels are rotated by 180° as indicated. (C) *T. thermophilus* RNAP (space-filling model) in complex with  $\sigma^{70}$  (ribbon model; PDB ID code 1IW7, Vassylyev et al. [2002]). In the  $\sigma^{70}$  model, the regions homologous to the DnaK and DnaJ binding site in  $\sigma^{32}$  and to the site destabilized by DnaJ are colored in green (hidden in RNAP), cyan, and dark blue. (D) Model of DnaK and DnaJ action in the regulation of  $\sigma^{32}$ . Upon release

the binding sites for DnaK and DnaJ within the folded  $\sigma^{32}$  and show that both chaperones influence the conformational stability of  $\sigma^{32}$ . Our data explain how the chaperone system regulates the activity of  $\sigma^{32}$  and how it could assist degradation of  $\sigma^{32}$  by the FtsH protease. We propose that the interaction of DnaK and DnaJ with  $\sigma^{32}$  exemplifies the general mode of action for Hsp70 systems in their interaction with natively folded protein clients. Our data give mechanistic insights into the mode of action of Hsp70 systems. Hsp70 and their DnaJ cochaperones bind to different sites in their client proteins. While Hsp70s bind to a site with a highly solvent accessible backbone, DnaJ cochaperones only interact with amino acid side chains. This study demonstrates that Hsp70 as well as its DnaJ cochaperone can influence the conformation of a bound protein substrate even at sites distant to the binding site. These observations may explain the ability of Hsp70 proteins to refold misfolded proteins and even to dissolve protein aggregates. They may also explain how Hsp70 proteins can regulate many signaling proteins in cooperation with Hsp90.

The identified DnaK-binding site consists of a hydrophobic core of four amino acids. In all  $\sigma^{32}$  homologs, the flanking regions are rich in hydrophilic and negatively charged residues. While these flanking segments do not promote DnaK binding, they may promote the surface exposure of the hydrophobic core residues, including their peptide backbone, thereby facilitating the enclosure of this site through binding into DnaK's substrate-binding cavity. A comparison of the affinities of DnaK to wild-type and mutant  $\sigma^{32}$  and to short 13-mer peptides comprising wild-type and mutant  $\sigma^{32}$  sequence suggests that the DnaK-binding site in  $\sigma^{32}$  is in an equilibrium between a closed and an open state and that the ratio between opening and closing rate depends on the hydrophobicity of the sequence (Supplemental Data). This conformational change between an open and closed state could be a rather local phenomenon, affecting mainly residues 189–201. It could also be part of the more global conformational equilibrium proposed by Darst and coworkers based on the comparison of the structures of FliA in complex with its anti- $\sigma$ -factor FlgM and  $\sigma^A$  in complex with RNAP (Sorenson and Darst, 2006; Sorenson et al., 2004). This analysis is substantiated by amide hydrogen exchange experiments, which demonstrate a rapid exchange of backbone amide hydrogens in this region, indicating an at least transient surface exposure in the native  $\sigma^{32}$  protein (Figure S5; Rist et al., 2003). In addition, the negative charges in the flanking segments may help to prevent aggregation of  $\sigma^{32}$  by electrostatic repulsion. It will be interesting to determine whether such a complex architecture is a more general feature of surface-exposed Hsp70-binding sites within native protein substrates.

We localized the DnaJ-binding site to the N-terminal domain of  $\sigma^{32}$  and provide evidence that residues 57–66 of  $\sigma^{32}$  are involved in binding. The DnaJ-binding site does not need to be unstructured, since DnaJ only distinguishes side chain hydrophobicity and, unlike DnaK, does not depend on backbone contacts (Rüdiger et al., 2001). In fact, structural modeling of  $\sigma^{32}$  revealed

that this region is part of the –10 promoter region recognition domain and exposes only a few hydrophobic side chains at the surface (Figure 5).

It might be argued that the site we identified is not the only DnaJ-binding site in  $\sigma^{32}$ , since the mutant proteins were still bound by DnaJ albeit with lower affinity. Since DnaJ binds to aromatic, hydrophobic, and positively charged side chains and not to the peptide backbone, it is possible that, unlike the DnaK-binding site, the DnaJ-binding site is not contiguous at the primary sequence, and side chains of neighboring structural elements distant in sequence might contribute to the binding site. Such a situation makes it very difficult to completely eliminate the binding site by point mutations. In addition, each amino acid replacement can have an effect on the structural stability of the protein. In fact, all  $\sigma^{32}$  variants with amino acid replacements in this region exhibited a higher propensity for aggregation, arguing for a tendency to locally unfold. Such local unfolding is likely to expose additional hydrophobic residues, which become new binding sites for DnaJ that in the wild-type protein are not accessible. Similarly, deletion of the N-terminal domain may have uncovered a new surrogate DnaJ-binding site obscuring the real magnitude of the effect on the DnaJ- $\sigma^{32}$  interaction. Since DnaJ evolved to bind to unfolded proteins, any mutations that increase the unfolding propensity will increase the affinity to DnaJ. The fact that our mutations decreased the affinity to DnaJ strongly argues that we indeed identified determinants for DnaJ binding.

Our experiments show that DnaK and DnaJ bind to distinct sites within native  $\sigma^{32}$ . For instance, we can exclude binding of DnaJ to the DnaK-binding site, since the DnaK-binding site is not a binding site for DnaJ at the primary sequence level (Figure S2) and mutational alterations in the DnaK-binding site expected to influence DnaJ binding do not lower the affinity of DnaJ to  $\sigma^{32}$  (Table 1). The fact that DnaK and DnaJ bind  $\sigma^{32}$  in different regions demonstrates that a direct transfer mechanism of the DnaJ-bound site into the substrate-binding cavity of DnaK is not operative in the case of  $\sigma^{32}$ . This mode of cooperation between DnaJ and DnaK might be more general, since a truncation and mutagenesis study on the native DnaK substrate RepA also suggests different binding sites for DnaK and DnaJ (Kim et al., 2002).

A rather surprising major finding of this study is that the binding of each of the two chaperones results in conformational changes within the substrate. We show that an Hsp70-bound substrate has a conformation distinct from the free substrate. In the presence of DnaJ,  $\sigma^{32}$  exchanged amide hydrogens with an overall higher rate, corresponding to a destabilization of the protein at two sites. One site is in close spatial vicinity to the DnaK-binding site in the model of the closed conformation of  $\sigma^{32}$  (modeled on  $\sigma^{28}$ ); the other destabilized site is in close vicinity to the DnaK-binding site in the primary structure (Figure 5). This suggests that DnaJ promotes an open conformation of  $\sigma^{32}$ , thereby facilitating DnaK binding. These data explain the synergism of DnaJ and  $\sigma^{32}$  in stimulating DnaK's ATPase activity and of DnaJ's high efficiency in loading  $\sigma^{32}$  onto DnaK.

---

from the RNAP,  $\sigma^{32}$  is in equilibrium between two conformational states with one being more unfolded. DnaJ shifts this equilibrium by binding to  $\sigma^{32}$ . The DnaK-binding site thus becomes more accessible. DnaK binds to  $\sigma^{32}$  hydrolyzing ATP by a  $\sigma^{32}$ - and DnaJ-stimulated mechanism. Binding of DnaK shifts the equilibrium to a still more exposed conformation of  $\sigma^{32}$ , thereby facilitating degradation of  $\sigma^{32}$  by FtsH.

DnaK binding also affects the conformation of  $\sigma^{32}$ . A segment in the N-terminal domain of  $\sigma^{32}$ , residues 31–49, shows in HX experiments more exchange in the presence of DnaK as compared to free  $\sigma^{32}$ . This region of  $\sigma^{32}$  is therefore less compact when  $\sigma^{32}$  is bound to DnaK, though the magnitude of this destabilization appears to be small. However, this destabilization is statistically highly significant, since we observed it in many single-point and time course experiments (p value from the time course experiment  $< 10^{-11}$ ) and also seems physiologically significant, since it is in the same magnitude as the most dramatic destabilizing amino acid replacement within an  $\alpha$  helix (alanine to proline). Furthermore, it is an underestimation due to technical reasons (loss of deuterons by pepsin cleavage).

How could the chaperones affect the conformation of  $\sigma^{32}$ ? There are principally two alternative ways. Chaperone binding could actively induce the conformational alteration in  $\sigma^{32}$ . Alternatively,  $\sigma^{32}$  could exist in at least two conformational states, a closed and an open state, which are in equilibrium with each other; chaperone binding could shift this equilibrium by binding to the open conformation. We favor the second alternative for the following reasons. First, amide hydrogen exchange is extremely rapid in many parts of  $\sigma^{32}$ , indicating a highly flexible protein or a protein that is in equilibrium between several different conformations (Rist et al., 2003, 2005). Second, DnaK can bind to  $\sigma^{32}$  in the absence of DnaJ. Since the crystal structure of the SBD of DnaK in complex with a substrate peptide demonstrates that the bound peptide stretch is in an extended conformation and must be at least 10 Å away from other parts of the substrate protein,  $\sigma^{32}$  must at least transiently exist in a conformation that allows such a binding. In addition, comparison between the affinity of DnaK to full-length  $\sigma^{32}$  and to a  $\sigma^{32}$ -derived peptide comprising the DnaK-binding site suggests an equilibrium between an open and a closed conformation. However, no matter in what way the chaperones effect the deprotection of amide hydrogens in  $\sigma^{32}$ , the result is the same: the ensemble of  $\sigma^{32}$  molecules is on average less stable.

The consequences of this destabilization for the regulation of this  $\sigma$ -factor are unclear. It is tempting to speculate that the conformational change in the N-terminal domain facilitates proteolysis of  $\sigma^{32}$  by FtsH, an AAA-protease known to degrade  $\sigma^{32}$  in vivo (Tatsuta et al., 1998) in a processive way from the N terminus to the C terminus (Okuno et al., 2004). However, FtsH lacks robust unfoldase activity and can degrade substrates only when they have low intrinsic thermodynamic stability (Herman et al., 2003). A chaperone-induced unfolding of a secondary structure element within the N domain may therefore facilitate degradation of  $\sigma^{32}$  in vivo (Figure 5D). Consistent with this idea are recent reports of  $\sigma^{32}$  mutants that are more stable in vivo (Obriest and Narberhaus, 2005; Yura et al., 2007). The stabilizing mutations (residues 47, 50, 51, 54, 83, 91, and 107) are located in the region where DnaJ binds (residues 57–66) and where the destabilization by DnaK (residues 31–49) and DnaJ (residues 91–101 and 158–175) occurs. Thus, this is a crucial region for the regulation of  $\sigma^{32}$ .

How could the DnaK-DnaJ system regulate the activity of  $\sigma^{32}$ ? Our data indicate that the DnaK-binding site is in close vicinity of, or identical with, a site involved in RNAP binding. This conclusion resides on two results. First,  $\sigma^{32}$  could be crosslinked to RNAP

through a UV-activated crosslinker located in the close neighborhood of the DnaK-binding site (data not shown). Second, mutational alterations within the DnaK-binding site reduced the affinity of RNAP to  $\sigma^{32}$  (Table 1). These results correlate well with the crystal structure of *T. thermophilus* RNAP holoenzyme, which shows that the region of  $\sigma^{70}$  corresponding to the DnaK-binding site in  $\sigma^{32}$  is enclosed between the  $\beta$  and  $\beta'$  subunit of RNAP (Figure 5C; Vassilyev et al., 2002). Consequently, DnaK and RNAP binding to this site are mutually exclusive, consistent with earlier observations (Gamer et al., 1996). In contrast, the DnaJ-binding site seems to be accessible, and DnaJ may be able to bind to  $\sigma^{32}$  even before it is released from the RNAP (Figure 5C). This would allow for a rapid targeting of  $\sigma^{32}$  to DnaK upon release from the RNAP.

This mechanism of regulation of the activity of  $\sigma$ -factors seems to be a more general scheme, as suggested by three recent crystal structures of complexes between  $\sigma$ -factors and their specific anti- $\sigma$ -factors (Campbell et al., 2002, 2003; Sorenson et al., 2004). Although the individual  $\sigma$ -factor/anti- $\sigma$ -factor pairs bind to each other in different ways, the effects are similar in that at least one binding determinant for RNAP becomes inaccessible. However, under equilibrium conditions, DnaK on its own cannot outcompete RNAP, neither in the ADP- nor in the ATP-bound state, since the dissociation equilibrium constant for the DnaK- $\sigma^{32}$  interaction is 1.4  $\mu$ M in the ADP state and at least 10-fold higher in the ATP state, while the  $K_D$  for RNAP is 12 nM. The efficient competitive binding of DnaK to  $\sigma^{32}$  relies on the high association rate in the ATP-bound state and subsequent rapid ATP hydrolysis that is coordinated by DnaJ, to take advantage of the low dissociation rate of the ADP-bound state. The thus calculated nonequilibrium  $K_D$  for the DnaK- $\sigma^{32}$  complex is in the low nM range. The effect of DnaJ on the interaction of DnaK with  $\sigma^{32}$  could therefore be 2-fold, as illustrated in the model of Figure 5D. First, the DnaK-binding site within  $\sigma^{32}$  becomes more accessible, increasing the association rate between DnaK and  $\sigma^{32}$ . Second, synergistic stimulation of ATP hydrolysis leads to an efficient trapping of  $\sigma^{32}$ . It will be important to determine whether this mode of action of the DnaK-DnaJ team is generally applicable for other substrates and for Hsp70 homologs.

## EXPERIMENTAL PROCEDURES

### Bacterial Strains and Plasmids

BB7142 was used for overexpression of  $\sigma^{32}$ . Site-directed mutagenesis was performed as described in Kunkel et al. (1991) using a pBluescriptKS+(*rho*H) construct. Deletion mutants were created by PCR.

### Proteins

$\sigma^{32}$  wild-type and mutants were purified as N- or C-terminally histidine-tagged variant (both fully complemented in vivo) as previously described (Arsène et al., 1999). RNAP, DnaK, and DnaJ were purified as published (Buchberger et al., 1994; Lowe et al., 1978; Schönfeld et al., 1995). C-terminally histidine-tagged DnaK was purified using Ni<sup>2+</sup>-NTA agarose (QIAGEN, Hilden, Germany) followed by ion exchange chromatography.

### In Vitro Experiments

<sup>3</sup>H labeling of proteins and analysis of protein interactions by gel filtration and SPR were performed as described previously (Arsène et al., 1999; Gamer et al., 1996) (Supplemental Data). Crosslinking experiments were performed

using cysteine specific crosslinker 4-(2-iodoacetamido) benzophenone (BPIA) bound to  $\sigma^{32}$ -S192C or  $\sigma^{32}$ -S205C mutants as described earlier (Arsène et al., 1999). ATPase assays were performed as described in Mayer et al. (1999).

#### Protease Assay

$\sigma^{32}$  protein (3  $\mu$ M) was incubated alone or in the presence of DnaK or DnaK-V436F (15  $\mu$ M) at 30°C for 2 hr, in 20  $\mu$ l final volume adjusted with protease buffer (10 mM Tris-HCl [pH 7.9], 2 mM CaCl<sub>2</sub>). Proteinase K (0.25  $\mu$ g/ml) or trypsin (2.5  $\mu$ g/ml) was added for 5 min, and the reaction was stopped by adding 1  $\mu$ l 200 mM PMSF. The samples were frozen for MALDI-TOF MS or completed with 20  $\mu$ l of Laemmli buffer (Laemmli, 1970) and boiled for SDS-PAGE on 15% acrylamide gels. Fragments were revealed by silver staining or transferred to polyvinylidene difluoride membranes (PVDF; Amersham-Pharmacia Biotech) for immunodetection using polyclonal anti- $\sigma^{32}$  antisera or for N-terminal sequencing. Immunoblots were developed by an immunofluorescence detection procedure using the Vistra ECF (Amersham-Pharmacia Biotech) and a fluorimaging system FLA2000 and MacBas software (Fuji Film Co.).

#### HX-MS Experiments

HX experiments were performed similarly to those described earlier (Rist et al., 2003). For the  $\sigma^{32}$ -DnaK-binding experiments, C-terminal histidine-tagged DnaK was immobilized on Poros 20AL beads (PerSeptive Biosystems) and packed into a 2 mm  $\times$  20 mm column. Immobilized DnaK was washed with 5 mM ATP diluted in HKM buffer containing 25 mM HEPES (pH 7.6), 50 mM KCl, and 5 mM MgCl<sub>2</sub>. After 10 min incubation, the excess of ATP was washed with HKM buffer. Under these conditions, all DnaK molecules on the column contain ATP. Thirty microliters of  $\sigma^{32}$  (10  $\mu$ M) were injected onto the column and incubated for at least 30 min at 30°C.  $\sigma^{32}$  thereby binds to DnaK in the ATP-bound open state and stimulates ATP hydrolysis, which leads to tight  $\sigma^{32}$  binding. The unbound  $\sigma^{32}$  was removed with HKM buffer. Amide hydrogen exchange was initiated by injection of D<sub>2</sub>O buffer containing 25 mM HEPES (pH 7.6), 50 mM KCl, and 5 mM MgCl<sub>2</sub> at 30°C. At various time points (10 s to 10 min), the exchange reaction was quenched and  $\sigma^{32}$  was eluted by injecting ice-cold quench buffer (400 mM KH<sub>2</sub>PO<sub>4</sub>/H<sub>3</sub>PO<sub>4</sub> [pH 2.2]). Eluted samples were injected into an HPLC setup and analyzed on an electrospray ionization-QTOF mass spectrometer. As an unbound control, Ni<sup>2+</sup>-NTA material was used instead of immobilized DnaK. In the case when DnaJ was included, 30  $\mu$ l of a solution containing  $\sigma^{32}$  (10  $\mu$ M), DnaJ (1  $\mu$ M), ATP (1 mM), and HKM buffer was injected onto the column containing immobilized DnaK and incubated for 20 min at 30°C. Unbound  $\sigma^{32}$ , DnaJ, and ATP were removed before the injection of D<sub>2</sub>O buffer.

For the  $\sigma^{32}$ -DnaJ-binding experiments, 60 pmol of  $\sigma^{32}$  was preincubated with 100 pmol of DnaJ or HKM buffer for 20 min at 30°C. Amide hydrogen exchange was initiated by a 20-fold dilution into D<sub>2</sub>O buffer at 30°C. The HX reaction was stopped at different time points (10 s to 1 min) with ice-cold quench buffer. Quenched samples were directly injected into our HPLC MS setup (see the Supplemental Data).

For the peptide-DnaJ binding experiments, 100 pmol of peptide was preincubated with 216 pmol of DnaJ or HKM buffer for 30 min at 30°C.

#### SUPPLEMENTAL DATA

The Supplemental Data include Supplemental Experimental Procedures, Supplemental References, seven figures, and two tables and can be found with this article online at [http://www.molecule.org/supplemental/S1097-2765\(08\)00693-X](http://www.molecule.org/supplemental/S1097-2765(08)00693-X).

#### ACKNOWLEDGMENTS

We would like to thank S. Druffel-Augustin and B. Zachmann-Brand for technical assistance. This work was supported by grants of the Deutsche Forschungsgemeinschaft (SFB638 to M.P.M., Leibnizprogram to B.B.) and the Fonds der Chemischen Industrie (to B.B.). W.R. was supported by a Kékulé Scholarship of the Fonds der Chemischen Industrie. F.A.-P. was supported by a Marie-Curie-Training Grant.

Received: July 16, 2007

Revised: April 23, 2008

Accepted: September 26, 2008

Published: November 6, 2008

#### REFERENCES

- Arsène, F., Tomoyasu, T., Mogk, A., Schirra, C., Schulze-Specking, A., and Bukau, B. (1999). Role of region C in regulation of the heat shock gene-specific sigma factor of *Escherichia coli*,  $\sigma^{32}$ . *J. Bacteriol.* *181*, 3552–3561.
- Blaber, M., Zhang, X.J., and Matthews, B.W. (1993). Structural basis of amino acid alpha helix propensity. *Science* *260*, 1637–1640.
- Buchberger, A., Schröder, H., Büttner, M., Valencia, A., and Bukau, B. (1994). A conserved loop in the ATPase domain of the DnaK chaperone is essential for stable binding of GrpE. *Nat. Struct. Biol.* *1*, 95–101.
- Bukau, B. (1993). Regulation of the *E. coli* heat shock response. *Mol. Microbiol.* *9*, 671–680.
- Campbell, E.A., Masuda, S., Sun, J.L., Muzzin, O., Olson, C.A., Wang, S., and Darst, S.A. (2002). Crystal structure of the *Bacillus stearotherophilus* anti-sigma factor SpoIIAB with the sporulation sigma factor sigmaF. *Cell* *108*, 795–807.
- Campbell, E.A., Tupy, J.L., Gruber, T.M., Wang, S., Sharp, M.M., Gross, C.A., and Darst, S.A. (2003). Crystal structure of *Escherichia coli* sigma(E) with the cytoplasmic domain of its anti-sigma RseA. *Mol. Cell* *11*, 1067–1078.
- Clarke, J., and Fersht, A.R. (1993). Engineered disulfide bonds as probes of the folding pathway of barnase: increasing the stability of proteins against the rate of denaturation. *Biochemistry* *32*, 4322–4329.
- Gamer, J., Bujard, H., and Bukau, B. (1992). Physical interaction between heat shock proteins DnaK, DnaJ, and GrpE and the bacterial heat shock transcription factor sigma 32. *Cell* *69*, 833–842.
- Gamer, J., Multhaupt, G., Tomoyasu, T., McCarty, J.S., Rudiger, S., Schonfeld, H.J., Schirra, C., Bujard, H., and Bukau, B. (1996). A cycle of binding and release of the DnaK, DnaJ and GrpE chaperones regulates activity of the *Escherichia coli* heat shock transcription factor sigma32. *EMBO J.* *15*, 607–617.
- Gross, C.A. (1996). Function and regulation of the heat shock proteins. In *Escherichia coli and Salmonella*, F.C. Neidhardt, ed. (Washington, D.C.: ASM Press), pp. 1382–1399.
- Grossman, A.D., Straus, D.B., Walter, W.A., and Gross, C.A. (1987).  $\sigma^{32}$  synthesis can regulate the synthesis of heat shock proteins in *Escherichia coli*. *Genes Dev.* *1*, 179–184.
- Han, W., and Christen, P. (2003). Mechanism of the targeting action of DnaJ in the DnaK molecular chaperone system. *J. Biol. Chem.* *278*, 19038–19043.
- Herman, C., Thévenet, D., D'Ari, R., and Bouloc, P. (1995). Degradation of sigma 32, the heat shock regulator in *Escherichia coli*, is governed by HflB. *Proc. Natl. Acad. Sci. USA* *92*, 3516–3520.
- Herman, C., Prakash, S., Lu, C.Z., Matouschek, A., and Gross, C.A. (2003). Lack of a robust unfoldase activity confers a unique level of substrate specificity to the universal AAA protease FtsH. *Mol. Cell* *11*, 659–669.
- Hoofnagle, A.N., Resing, K.A., and Ahn, N.G. (2003). Protein analysis by hydrogen exchange mass spectrometry. *Annu. Rev. Biophys. Biomol. Struct.* *32*, 1–25.
- Horovitz, A., Matthews, J.M., and Fersht, A.R. (1992). Alpha-helix stability in proteins. II. Factors that influence stability at an internal position. *J. Mol. Biol.* *227*, 560–568.
- Kanemori, M., Yanagi, H., and Yura, T. (1999). Marked instability of the  $\sigma^{32}$  heat shock transcription factor at high temperature. *J. Biol. Chem.* *274*, 22002–22007.
- Karzai, A.W., and McMacken, R. (1996). A bipartite signaling mechanism involved in DnaJ-mediated activation of the *Escherichia coli* DnaK protein. *J. Biol. Chem.* *271*, 11236–11246.
- Kim, S.Y., Sharma, S., Hoskins, J.R., and Wickner, S. (2002). Interaction of the DnaK and DnaJ chaperone system with a native substrate, P1 RepA. *J. Biol. Chem.* *277*, 44778–44783.

- Kunkel, T.A., Bebenek, K., and McClary, J. (1991). Efficient site-directed mutagenesis using uracil-containing DNA. *Methods Enzymol.* **204**, 125–139.
- Laemmli, U.K. (1970). Cleavage of structural proteins during the assembly of the head of bacteriophage T4. *Nature* **227**, 680–685.
- Laufen, T., Mayer, M.P., Beisel, C., Klostermeier, D., Reinstein, J., and Bukau, B. (1999). Mechanism of regulation of Hsp70 chaperones by DnaJ co-chaperones. *Proc. Natl. Acad. Sci. USA* **96**, 5452–5457.
- Li, J., Qian, X., and Sha, B. (2003). The crystal structure of the yeast Hsp40 Ydj1 complexed with its peptide substrate. *Structure (Camb.)* **11**, 1475–1483.
- Liberek, K., Galitski, T.P., Zyllicz, M., and Georgopoulos, C. (1992). The DnaK chaperone modulates the heat shock response of *Escherichia coli* by binding to the  $\sigma^{32}$  transcription factor. *Proc. Natl. Acad. Sci. USA* **89**, 3516–3520.
- Liberek, K., Wall, D., and Georgopoulos, C. (1995). The DnaJ chaperone catalytically activates the DnaK chaperone to preferentially bind the  $\sigma^{32}$  heat shock transcriptional regulator. *Proc. Natl. Acad. Sci. USA* **92**, 6224–6228.
- Lowe, P.A., Hager, D.A., and Burgess, R.R. (1978). Purification and properties of the  $\sigma$  subunit of *Escherichia coli* DNA-dependent RNA polymerase. *Biochemistry* **18**, 1344–1352.
- Mayer, M.P., Laufen, T., Paal, K., McCarty, J.S., and Bukau, B. (1999). Investigation of the interaction between DnaK and DnaJ by surface plasmon resonance spectroscopy. *J. Mol. Biol.* **289**, 1131–1144.
- Mayer, M.P., Schröder, H., Rüdiger, S., Paal, K., Laufen, T., and Bukau, B. (2000). Multistep mechanism of substrate binding determines chaperone activity of Hsp70. *Nat. Struct. Biol.* **7**, 586–593.
- McCarty, J.S., Rüdiger, S., Schönfeld, H.-J., Schneider-Mergener, J., Nakahigashi, K., Yura, T., and Bukau, B. (1996). Regulatory region C of the *E. coli* heat shock transcription factor,  $\sigma^{32}$ , constitutes a DnaK binding site and is conserved among eubacteria. *J. Mol. Biol.* **256**, 829–837.
- Obrist, M., and Narberhaus, F. (2005). Identification of a turnover element in region 2.1 of *Escherichia coli* sigma32 by a bacterial one-hybrid approach. *J. Bacteriol.* **187**, 3807–3813.
- Okuno, T., Yamada-Inagawa, T., Karata, K., Yamanaka, K., and Ogura, T. (2004). Spectrometric analysis of degradation of a physiological substrate sigma32 by *Escherichia coli* AAA protease FtsH. *J. Struct. Biol.* **146**, 148–154.
- O'Neil, K.T., and DeGrado, W.F. (1990). A thermodynamic scale for the helix-forming tendencies of the commonly occurring amino acids. *Science* **250**, 646–651.
- Peitsch, M.C. (1996). ProMod and Swiss-Model: internet-based tools for automated comparative protein modelling. *Biochem. Soc. Trans.* **24**, 274–279.
- Rist, W., Jørgensen, T.J.D., Roepstorff, P., Bukau, B., and Mayer, M.P. (2003). Mapping temperature-induced conformational changes in the *Escherichia coli* heat shock transcription factor sigma 32 by amide hydrogen exchange. *J. Biol. Chem.* **278**, 51415–51421.
- Rist, W., Rodriguez, F., Jørgensen, T.J., and Mayer, M.P. (2005). Analysis of subsecond protein dynamics by amide hydrogen exchange and mass spectrometry using a quenched-flow setup. *Protein Sci.* **14**, 626–632.
- Rüdiger, S., Germeroth, L., Schneider-Mergener, J., and Bukau, B. (1997). Substrate specificity of the DnaK chaperone determined by screening cellulose-bound peptide libraries. *EMBO J.* **16**, 1501–1507.
- Rüdiger, S., Schneider-Mergener, J., and Bukau, B. (2001). Its substrate specificity characterizes the DnaJ cochaperone as a scanning factor for the DnaK chaperone. *EMBO J.* **20**, 1042–1050.
- Rüdiger, S., Schneider-Mergener, J., and Bukau, B. (2001). Its substrate specificity characterizes the DnaJ chaperone as scanning factor for the DnaK chaperone. *EMBO J.* **20**, 1–9.
- Schönfeld, H.-J., Schmidt, D., and Zulauf, M. (1995). Investigation of the molecular chaperone DnaJ by analytical ultracentrifugation. *Prog. Colloid Polym. Sci.* **99**, 7–10.
- Sorenson, M.K., and Darst, S.A. (2006). Disulfide cross-linking indicates that FigM-bound and free sigma28 adopt similar conformations. *Proc. Natl. Acad. Sci. USA* **103**, 16722–16727.
- Sorenson, M.K., Ray, S.S., and Darst, S.A. (2004). Crystal structure of the flagellar sigma/anti-sigma complex sigma(28)/FigM reveals an intact sigma factor in an inactive conformation. *Mol. Cell* **14**, 127–138.
- Straus, D.B., Walter, W.A., and Gross, C.A. (1987). The heat shock response of *E. coli* is regulated by changes in the concentration of  $\sigma^{32}$ . *Nature* **329**, 348–350.
- Straus, D., Walter, W., and Gross, C.A. (1990). DnaK, DnaJ, and GrpE heat shock proteins negatively regulate heat shock gene expression by controlling the synthesis and stability of  $\sigma^{32}$ . *Genes Dev.* **4**, 2202–2209.
- Tatsuta, T., Tomoyasu, T., Bukau, B., Kitagawa, M., Mori, H., Karata, K., and Ogura, T. (1998). Heat shock regulation in the *ftsH* null mutant of *Escherichia coli*: dissection of stability and activity control mechanisms of sigma32 *in vivo*. *Mol. Microbiol.* **30**, 583–593.
- Tilly, K., McKittrick, N., Zyllicz, M., and Georgopoulos, C. (1983). The DnaK protein modulates the heat-shock response of *Escherichia coli*. *Cell* **34**, 641–646.
- Tilly, K., Spence, J., and Georgopoulos, C. (1989). Modulation of stability of the *Escherichia coli* heat shock regulatory factor sigma 32. *J. Bacteriol.* **171**, 1585–1589.
- Tomoyasu, T., Gamer, J., Bukau, B., Kanemori, M., Mori, H., Rutman, A.J., Oppenheim, A.B., Yura, T., Yamanaka, K., Niki, H., et al. (1995). *Escherichia coli* FtsH is a membrane-bound, ATP-dependent, protease which degrades the heat-shock transcription factor sigma 32. *EMBO J.* **14**, 2551–2560.
- Vassilyev, D.G., Sekine, S., Laptenko, O., Lee, J., Vassilyeva, M.N., Borukhov, S., and Yokoyama, S. (2002). Crystal structure of a bacterial RNA polymerase holoenzyme at 2.6 Å resolution. *Nature* **417**, 712–719.
- Wetzel, R., Perry, L.J., Baase, W.A., and Becktel, W.J. (1988). Disulfide bonds and thermal stability in T4 lysozyme. *Proc. Natl. Acad. Sci. USA* **85**, 401–405.
- Yura, T., and Nakahigashi, K. (1999). Regulation of the heat-shock response. *Curr. Opin. Microbiol.* **2**, 153–158.
- Yura, T., Guisbert, E., Poritz, M., Lu, C.Z., Campbell, E., and Gross, C.A. (2007). Analysis of sigma32 mutants defective in chaperone-mediated feedback control reveals unexpected complexity of the heat shock response. *Proc. Natl. Acad. Sci. USA* **104**, 17638–17643.
- Zhu, X., Zhao, X., Burkholder, W.F., Gragerov, A., Ogata, C.M., Gottesman, M., and Hendrickson, W.A. (1996). Structural analysis of substrate binding by the molecular chaperone DnaK. *Science* **272**, 1606–1614.